Am J Transl Res 2022;14(11):8166-8174
www.ajtr.org /ISSN:1943-8141/AJTR0146199

Original Article

Identification of crucial genes that induce coronary atherosclerosis through endothelial cell dysfunction in AMI-identifying hub genes by WGCNA

Sentong Xiao, Chunyan Kuang

Department of Cardiovascular Diseases, Guizhou Provincial People's Hospital, Nanming District, Guiyang 550003, Guizhou, People's Republic of China

Received August 29, 2022; Accepted October 30, 2022; Epub November 15, 2022; Published November 30, 2022

Abstract: Objective: To identify the most relevant genes of cardiovascular disease in acute myocardial infarction patients using weighted gene co-expression network analysis (WGCNA). Methods: The microarray dataset of GSE66360 was downloaded from the Gene Expression Omnibus (GEO) website. The differential genes with adjusted $P < 0.05$ and $|\log2 \text{ fold change (FC)}| > 0.5$ were included in the analysis. The weighed gene co-expression network analysis (WGCNA) was used to build a gene co-expression network and identify the most significant module. Cytoscape was used to filter the hub genes. Gene Ontology (GO) and Kyoto Encyclopedia of Genes and Genomes (KEGG) pathway enrichment analyses were performed for the hub genes. The key genes were defined as having high statistical and biological significance. Results: A total of 4751 differentially expressed genes (DEGs) were screened from the dataset. The purple module had the highest significance in AMI. There were 47 hub genes identified from the module. The GO terms "amyloid beta protein metabolism" and "carbohydrate metabolism" and the KEGG terms "phagosome-related pathways" and "Staphylococcus aureus-associated pathways" were the pathways strongly enriched in AMI. Fatty acid translocase cluster of differentiation (CD36), formyl peptide receptor type 2 (FPR2), integrin subunit alpha M (ITGAM), and oxidized low density lipoprotein receptor 1 (OLR1) were considered key genes in AMI. Conclusion: Our research suggested that the underlying mechanism was related to inflammation and lipid formation. The hub genes identified were CD36, FPR2, ITGAM, and OLR1.

Keywords: Acute myocardial infarction, endothelial cells, hub genes, significant modules

Introduction

An acute myocardial infarction (AMI) continues to be the major cause of death worldwide [1]. The lack of supporting data for this diagnosis prohibits us from making an accurate and timely death prediction [2]. We need to find other ways to make timely predictions and diagnoses of coronary artery disease, through gene prediction, for example. Increasing evidence has shown that endothelial cells (ECs) influence the initiation of inflammation and cellular repair upon vascular injury [3, 4]. The interaction mechanisms of various biological processes in ECs remain unclear, especially those connected with gene ontology and gene pathways.

Vascular endothelial growth factor (VEGF) has an important proangiogenic effect on Ecs [5], which is regulated by receptor 2 (VEGFR-2). Recent studies have shown that forkhead box O1 (FoxO1) regulates VEGF expression by influencing transcription to achieve an antioxidant function [6, 7]. The expression of CD36 can be positively correlated with coronary atherosclerosis [8, 9]. Formyl peptide receptor (FPR) signaling produces high levels of reactive oxygen species (ROS) [10, 11]. Oxidized low-density lipoprotein receptor-1 (LOX-1) levels are significantly associated with oxidative stress [12]. All these factors are promising targets to study.

Previous gene-based studies on this topic have focused on differential gene expression. Few studies have considered the relationship between gene expression and clinical characteristics. Weighted gene co-expression network analysis (WGCNA) can be used as a bioinfor-

matics approach for exploring the relationship between different genes or gene clusters and clinical characteristics. WGCNA is widely used to analyze microarray data, particularly for identifying functional modules. In 2019, Yang & Li identified CD36 as a hub gene in the pathogenesis of lupus nephritis and showed that CD36 plays an important role in the activation of neutrophils and the regulation of immune function by using WGCNA [13]. This finding indicated that WGCNA can be used to identify hub genes in microarray data. An mRNA expression profile from a gene microarray analysis of AMI samples was used to identify highly connected hub genes and important modules. To explore the molecular pathways involved in AMI, we used WGCNA to construct a co-expression network and identify significant modules in the network. Weighted gene co-expression networks can be used to relate functions of unknown genes with biological processes. Disease-relevant genes were selected and ranked according to gene correlations.

Materials and methods

Microarray data

Microarray data for AMI (GSE66360) [14] were downloaded from the Gene Expression Omnibus, including data from circulating EC samples from AMI patients (n = 49) and controls (n = 50).

Methods

Differential expression analysis: Limma is an R software package that analyzes data from biological experiments. It has been significantly expanded for analyzing RNA sequencing (RNA-seq) data, with enhanced possibilities for the biological interpretation of gene expression differences. We used limma to select genes with a |log2 fold change (FC)| > 0.5 and adjusted P < 0.05 as differentially expressed genes (DEGs) [15].

WGCNA: We calculated Pearson's correlation matrices for all pairs of genes and defined the correlation coefficient between genes m and n as Smn = cor (m, n). We used the power function amn = power (Smn, β) = |Smn| β to transform the Pearson correlation matrix into a connection strength matrix. This step can recognize strong correlations and reduce the impact of weak correlations at the exponential level. We selected a power of β = 14 (Soft. R. sq = 0. 9) to ensure that we could obtain a scale-free network. These connection strengths were used to calculate topological overlap. This is a measure of the connectivity of a pair of genes. WGCNA can be used to identify highly related gene modules and summarize these clusters using intrinsic or centered genes in the module. It can be employed to correlate modules with each other and with external sample characteristics (using the intrinsic gene network approach) and to calculate eligibility measures for members in the module. The related network facilitates a network-based genetic screening approach that can be used to identify candidate biomarkers or therapeutic targets [16].

We selected the genes in the module to generate a network structure diagram through STRING PPI analysis and removed all free genes. The remaining genes were imported into Cytoscape to select hub genes by using the MCODE plug-in. Gene Ontology (GO) and GSEE annotations were performed. The GO analysis divided the functions of gene mechanisms into three major categories: biological processes (BP), cellular components (CC), and molecular functions (MF). The Kyoto Encyclopedia of Genes and Genomes (KEGG) pathway database was used to describe the functions of molecules or genes.

Results

Differential expression analysis of enriched ECs from AMI patients and controls

A total of 54,676 genes were obtained from 99 samples (49 AMI patients and 50 controls) after data preprocessing. We chose a |log fold change| > 0.5 and adjusted P < 0.05 as the criteria for identifying DEGs. A total of 4751 DEGs were identified for subsequent analysis under the same criteria (heatmap and volcano plot shown in **Figure 1**). We correlated these results with sample traits. The clustering results are shown in **Figure 2**.

Identification of key modules by WGCNA

The WGCNA package in R software was used [17, 18]. DEGs with similar expression patterns

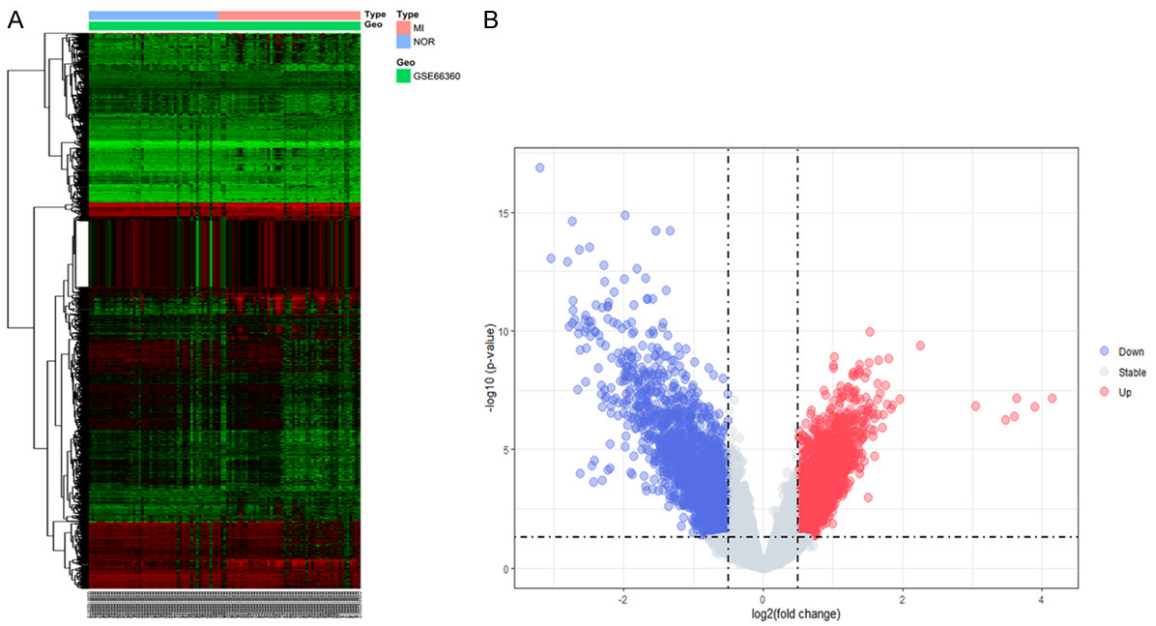

Figure 1. Heatmap and volcano plot of differential gene expression. A heatmap and volcano plot of 4751 differentially expressed genes were constructed, and a |log fold change| > 0.5 and adjusted P < 0.05 were chosen as criteria for differentially expressed genes. A. Heatmap of differentially expressed genes with significant consistency. Red represents upregulated genes. Green represents downregulated genes. B. Volcano plot based on the specified criteria. Red indicates genes that are upregulated. Blue indicates genes that are downregulated.

were grouped into different modules by hierarchical average linkage clustering. A total of 20 modules were identified. The correlations between the disease and the module traits were calculated. The related table of matrix trait data was imported into the R language and correlated with the gene expression matrix (GS) and module membership (MM) (the gray part of **Figure 2** corresponds to uniform characteristics). Those modules with a higher GS_MM value were considered more relevant to the disease (**Figure 3**).

We found that among all selected modules, the purple and black modules showed the highest GS_MM values (purple r = 0.6, P = 6e-11, black r = 0.6, P = 4e-11). The magenta module presented some degree of correlation (r = 0.47, P = 9e-07). We selected the genes in the purple, black, and magenta modules and matched them with the calculated differential gene expression log fold changes. We screened out free genes on the https://string-db.org/website and used the remaining genes to generate a network structure map. We introduced the genes in the network. For Cytoscape analysis, the 47 most relevant genes were selected as the hub genes of the disease.

GO and KEGG enrichment analysis of trait-related modules

The 47 most relevant genes that were considered as the hub genes of the disease were annotated through GO and KEGG analysis (**Figure 4**). The most relevant GO annotations for the disease were the metabolism of amyloid β protein and the metabolism of carbohydrates (**Table 1**). The most relevant KEGG pathways were the phagosome and Staphylococcus aureus infection pathways (**Table 2**) (Detail is in the appendix with GO (Table S1) and KEGG (Table S2)). In the graphs of the GO and KEGG analysis results, the more red the color is, the higher the correlation. Blue represented a lower correlation. In the dot plot, the larger the point is, the more highly enriched the gene is. For the modules that we selected, we chose the color that was most relevant, and gene enrichment was relatively enriched. The identified GO terms were mainly related to the metabolism of amyloid beta protein and carbohydrate metabolism (**Figure 4**). It included terms such as “amyloid beta protein metabolism” (gene count = 5, P = 1.38e-06) and “carbohydrate metabolism” (gene count = 7, P = 4.31e-06). The main identified KEGG terms included “phagosome-related pathways” (gene count = 7, P = 9.42e-05) and

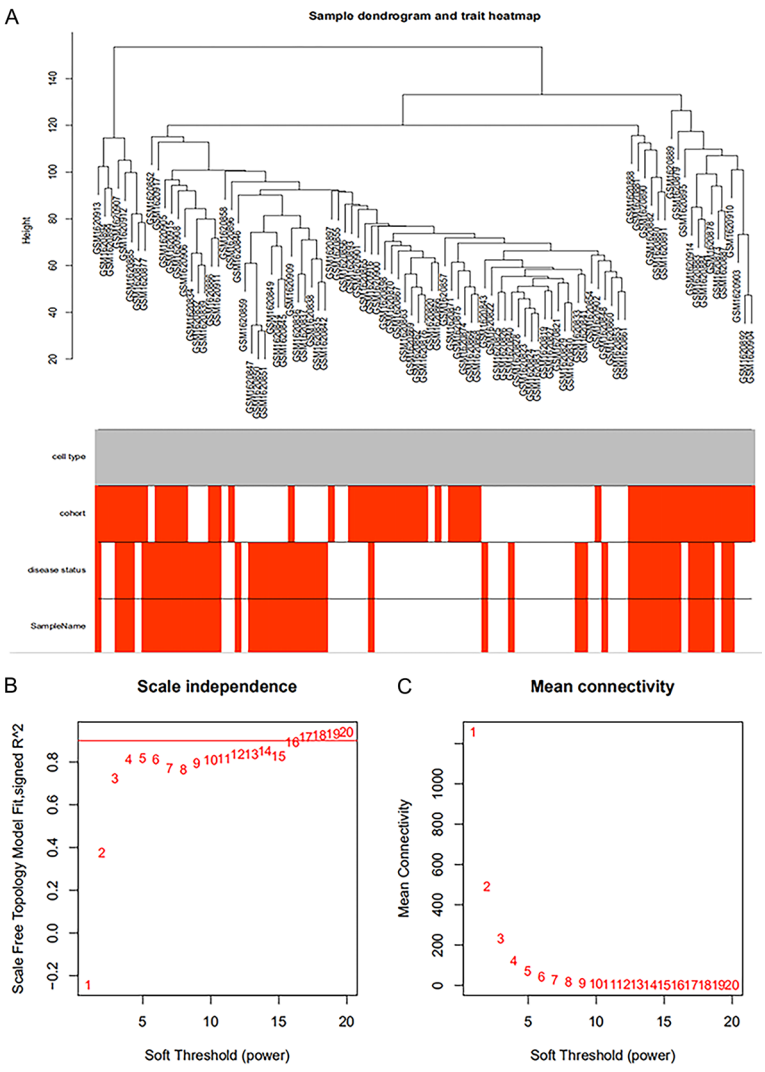

Figure 2. Sample cluster dendrogram and soft-thresholding value (β) estimation. A. The expression profile of 50 normal samples and 49 MI samples, the sample cluster dendrogram and the clinical characteristic (group of myocardial infarctions, red; controls, white) heat map. B. Scale-free fit index analysis for each β value from 1 to 20. C. Average connectivity analysis for each β value from 1 to 20. We chose β = 14 for subsequent analysis, because when the scale-free fitting index reached 0.85, the samples exhibited the highest average connectivity.

"Staphylococcus aureus-associated pathways" (gene count = 5, P = 3.01e-05). We identified that the genes formyl peptide receptor 2 (FPR2), integrin alpha M (ITGAM), and CD36 were related to "amyloid beta protein metabolism". Oxidized low density lipoprotein receptor 1 (OLR1) and CD33 were related to "carbohydrate metabolism". OLR1, ITGAM, and CD36 were related to "phagosome-related pathways". FPR2, ITGAM, and CAMP were related to "Staphylococcus aureus-associated pathways". In summary, four genes (FPR2, OLR1, ITGAM, and CD36) were repeatedly identified as key molecules by sub-pathway screening and data mining.

Discussion

Endothelial cells (ECs) within the luminal surfaces of blood vessels serve multiple functions, such as supporting tissue barrier function and promoting the transport of molecules and cells [19]. Coronary heart disease (CHD) is caused by vascular endothelial injury and poor repair after injury. Those processes are relevant to oxidative stress and vascular inflammation [20, 21]. The hub genes and pathways we found were involved with those factors. Our results showed that fatty acid translocase cluster of differentiation (CD36) is a key gene in the development of coronary heart disease. CD36 has been proven to play a role in diseases such as stroke, coronary atherosclerosis, and Alzheimer's syndrome [22-24]. CD36 is a membrane glycoprotein that is found in various cell types, such as monocytes, macrophages, microvascular ECs, adipocytes, and platelets [25-28]. CD36 can act as a transporter or receptor of biologically active lipids to regulate the metabolism of lipids, glucose, and proteins. It affects the formation of amyloid aggregates that can cause damage in cardiovascular and cerebrovascular diseases. As a result, it associates with coronary heart disease and Alzheimer's disease [29, 30]. CD36 macrophages participate in the formation of atherosclerotic arterial lesions by interacting with oxLDL, triggering a signal cascade of inflammatory responses [31]. CD36 plays a role in oxLDL uptake and foam cell formation, which is the initial critical stage of atherosclerosis [32].

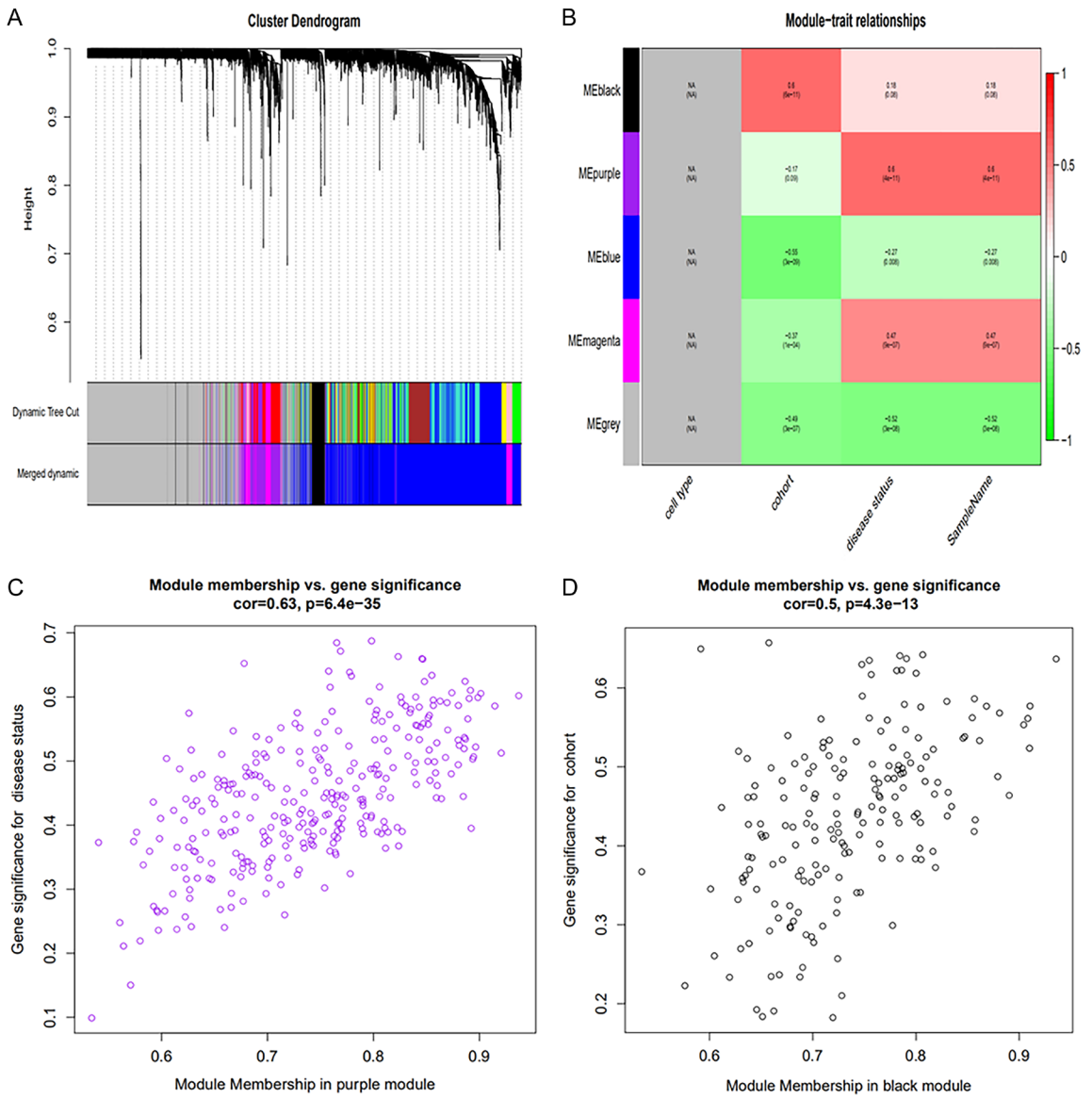

Figure 3. Division and validation of co-expression modules. A. Tree diagram dividing all genes into 20 modules based on the dissimilarity measure (1-TOM). Color-coded modules are indicated below the tree. The upper portion shows the original division according to average link hierarchical clustering based on the TOM-based similarity measure. The lower portion is a module involving merging according to Pearson feature gene correlation. B. Result of calculating the feature correlation coefficient of the module. The redder the color is, the higher the correlation between upregulated gene expression and the disease in this module. Gray indicates no correlation. C and D. Scatter plots of genes in the pink and black plates and the correlation between GS and MM in the module. The specific values are as follows: purple (cor = 0.63, P = 6.4e-35) and black (cor = 0.5, P = 4.3e-13).

CD36 can promote vascular amyloid deposition during the development of Alzheimer's disease, leading to cerebrovascular damage, neurovascular dysfunction, cognitive deficits, and increased uptake of fatty acids by M2 phagocytes [31, 33]. CD36 plays a positive role in absorbing pathogens, triggering immune responses, phagocytosing nonpathogenic modified proteins, inhibiting angiogenesis, and downregulating immune responses when inflammation subsides [34, 35].

We found that integrin subunit alpha M (ITGAM) was involved in AMI. There are few reports concerning ITGAM. ITGAM acts as a conduction factor and triggering receptor in the pathogen-

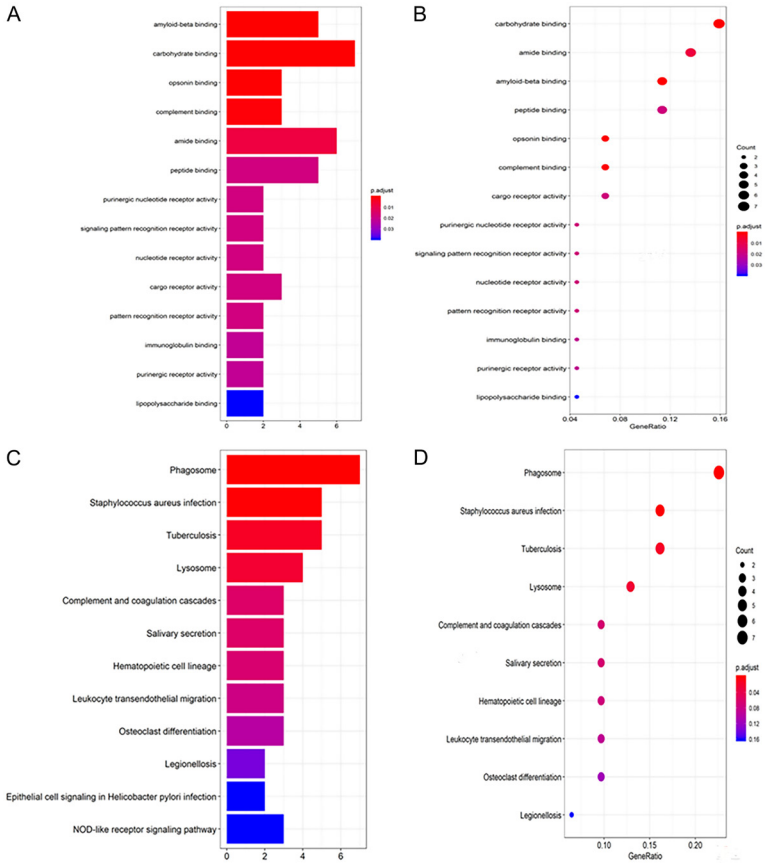

Figure 4. GO enrichment analyses and KEGG enrichment analyses of hub genes. A and B. Histograms and scatter plots of GO annotations; C and D. Histograms and scatter plots of KEGG annotations. In the histogram plots, the depth of color corresponds to the significance of the enrichment of each term, and the x-axis indicates the enriched gene count. The depth of color corresponds to the significance of the enrichment of each term. The size of the circle indicates the enriched gene count in the scatter plots.

esis of inflammation. It can cause inflammation that is associated with certain bacteria through a noncanonical form of autophagy. This is referred to as LC3-associated phagocytosis [36]. ITGAM is involved in diseases, such as systemic lupus erythematosus (SLE) and systemic sclerosis, as a component of the intermediate onset process [37]. ITGAM stimulates the pathogenesis of SLE by mediating the impairment of phagocyte function and acts as a conduction factor in the development of inflammation [38, 39]. The role of ITGAM in the pathogenesis of AMI is unclear.

An oxidized LDL receptor-1 (OLR1) was shown to be involved in the pathogenesis of AMI in our study. OLR1 can be involved in the occurrence of myocardial infarction through the following mechanisms. OLR1 shows a proinflammatory effect in cardiovascular disease and mediates the absorption and binding of oxLDL by vascular cells in atherosclerotic lesions. Increased expression of OLR1 promotes the increases in serum IL17 level and Th17 cells. These changes positively promote initial lesion formation in atherosclerotic cells. OLR1 encodes the lectin-like oxidized LDL receptor (LOX-1). It is expressed in vascular ECs and is found in macrophages, platelets, and smooth muscle cells. The combination of LOX-1 and LDL leads to EC dysfunction, forming primary atherosclerotic lesions.

Our research showed that formyl peptide receptor type 2 (FPR2) genes play an important role in AMI. FPRs are members of the G protein-coupled receptor (GPCR) family and have been proven to promote inflammation and immune responses. Human FPRs include three members: FPR1, FPR2, and FPR3. In humans, a series of activators, such as serum amyloid A (SSA) and glucocorticoid-induced annexin 1, bind FPR2. This was associated with chronic inflammation and amyloidosis [40]. SSA upregulates the expression levels of inflammatory mediators, such as cytokines, chemokines, and ROS [41]. It was found that a reduction in FPR2 can reduce the occurrence of airway allergic inflammation. In mouse experiments, FPR2 has been shown to promote M1 macrophage polarization and antitumor host responses. These findings show that FPR2 can participate in myeloid cell development and mediate leukocyte chemotaxis [42]. Petri et al. found that compared with healthy blood vessels, FPR2 mRNA levels in human samples with atherosclerotic lesions were upregulated. In contrast, lacking FPR2 can activate macrophages at coronary artery lesions and reduce monocyte infiltration and foam cell formation. This hinders the development of coronary atherosclerotic plaques [43]. These results showed that the expression of FPR2

Table1. GO description

ID	Description	*P* value	gene ID
GO: 0001540	amyloid-beta binding	1. 39E-06	CD36/LILRB2/FPR2/CST3/ITGAM
GO: 0030246	carbohydrate binding	4. 31E-06	CLEC4D/MGAM/PTX3/CD33/CD93/CLEC12A/OLR1
GO: 0001846	opsonin binding	6. 39E-06	PTX3/CD93/ITGAM
GO: 0001848	complement binding	1. 85E-05	PTX3/CD93/ITGAM
GO: 0033218	amide binding	0. 000235222	CD36/FPR2/ITGAM/OLR1
GO: 0042277	peptide binding	0. 000793511	CD36/LILRB2/FPR2/CST3/ITGAM/FOLR3
GO: 0001614	purinergic nucleotide receptor activity	0. 001115673	CD36/OLR1
GO: 0008329	signaling pattern recognition receptor activity	0. 001115673	CD36/OLR1
GO: 0016502	nucleotide receptor activity	0. 001115673	PPBP/CXCL1
GO: 0038024	cargo receptor activity	0. 001228596	CD36/LILRB2/FPR2/CST3/ITGAM
GO: 0038187	pattern recognition receptor activity	0. 001231166	P2RX1/PTAFR
GO: 0019865	immunoglobulin binding	0. 001610459	P2RX1/PTAFR
GO: 0035586	purinergic receptor activity	0. 001747738	CD36/PTAFR
GO: 0001530	lipopolysaccharide binding	0. 00341212	FCAR/FCER1G

Table 2. KEGG description

ID	Description	*P* value	gene ID
hsa04145	Phagosome	1. 24E-06	CD36/FCAR/ITGAM/ATP6V0C/CTSS/CYBB/OLR1
hsa05150	Staphylococcus aureus infection	2. 73E-05	FCAR/FPR2/ITGAM/CAMP/PTAFR
hsa05152	Tuberculosis	0. 000531272	FCER1G/ITGAM/ATP6V0C/CTSS/CAMP
hsa05417	Lipid and atherosclerosis	0. 001186983	CD36/CXCL1/CYBB/OLR1/MMP9
hsa04142	Lysosome	0. 001477046	SLC11A1/ASAH1/ATP6V0C/CTSS

can be correlated with coronary atherosclerotic plaque lesions.

In conclusion, a total of 4751 DEGs and 15 modules were identified in the CAD samples. Through analysis of the first 47 genes showing the highest connectivity in important modules, FPR2, OLR1, ITGAM, and CD36 were identified as targets for the treatment of CAD. The 2 KEGG pathways and 2 GO processes with the most relevance to inflammation and lipid formation were established. All these factors are connected with the cellular oxidation process, suggesting that we need to identify therapeutic targets in related pathways. We identified the factors in endothelial cells that can be associated with the pathogenesis of AMI. We hope to provide more clues to develop new diagnostic and therapeutic strategies of AMI. The lack of functional experiments was a limitation of this work. More research is required to assess the regulatory and expression of these genes and pathways.

Acknowledgements

We thank Bairong Shen for his kind help in this work. This study was supported mainly by funding from the Guizhou Science and Technology Department (Grant Qian-Ke-He [2018] 1097), the National Natural Science Foundation of China (No. 81560056), Program for Training Outstanding Young Scientific and Technological Talents of Guizhou Province (No. Qian Kehe Platform Talents [2019] 5662), Program for the Scientific Activities of Selected Returned Overseas Professionals in Guizhou Province (Grant Qian-ren [2018] 0003). Guizhou Science and Technology Platform and Talent Team Planning Project (QKHPTRC [2017] 5405).

Disclosure of conflict of interest

None.

Address correspondence to: Chunyan Kuang, Department of Cardiovascular Diseases, Guizhou Provincial People's Hospital, Nanming District, Guiyang 550003, Guizhou, People's Republic of China. Tel: +86-13007804567; Fax: +86-0851885603809; E-mail: xiaokcy@sina.com

References

[1] Zorov DB, Juhaszova M and Sollott SJ. Mitochondrial reactive oxygen species (ROS)

and ROS-induced ROS release. Physiol Rev 2014; 94: 909-950.
[2] Svendsen MT, Bøggild H, Skals RK, Mortensen RN, Kragholm K, Hansen SM, Riddersholm SJ, Nielsen G and Torp-Pedersen C. Uncertainty in classification of death from fatal myocardial infarction: a nationwide analysis of regional variation in incidence and diagnostic support. PLoS One 2020; 15: e0236322.
[3] Al-Soudi A, Kaaij MH and Tas SW. Endothelial cells: from innocent bystanders to active participants in immune responses. Autoimmun Rev 2017; 16: 951-962.
[4] Ghose S, Biswas S, Datta K and Tyagi RK. Dynamic Hyaluronan drives liver endothelial cells towards angiogenesis. BMC Cancer 2018; 18: 648.
[5] Ballmer-Hofer K. Vascular endothelial growth factor, from basic research to clinical applications. Int J Mol Sci 2018; 19: 3750.
[6] Jeon HH, Yu Q, Lu Y, Spencer E, Lu C, Milovanova T, Yang Y, Zhang C, Stepanchenko O, Vafa RP, Coelho PG and Graves DT. FOXO1 regulates VEGFA expression and promotes angiogenesis in healing wounds. J Pathol 2018; 245: 258-264.
[7] Yan D, He Y, Dai J, Yang L, Wang X and Ruan Q. Vascular endothelial growth factor modified macrophages transdifferentiate into endothelial-like cells and decrease foam cell formation. Biosci Rep 2017; 37: BSR20170002.
[8] Wu J, He Z, Gao X, Wu F, Ding R, Ren Y, Jiang Q, Fan M, Liang C and Wu Z. Oxidized high-density lipoprotein impairs endothelial progenitor cells' function by activation of CD36-MAPK-TSP-1 pathways. Antioxid Redox Signal 2015; 22: 308-324.
[9] Soria-Florido MT, Schröder H, Grau M, Fitó M and Lassale C. High density lipoprotein functionality and cardiovascular events and mortality: a systematic review and meta-analysis. Atherosclerosis 2020; 302: 36-42.
[10] Jabarpour M, Rashtchizadeh N, Ghorbani Haghjo A, Argani H, Nemati M, Dastmalchi S, Roshangar L, Ranjbarzadhag M, Mesgari-Abbasi M, Bargahi N and Sanajou D. Protection of renal damage by HMG-CoA inhibitors: a comparative study between atorvastatin and rosuvastatin. Iran J Basic Med Sci 2020; 23: 206-213.
[11] Leoni G, Alam A, Neumann PA, Lambeth JD, Cheng G, McCoy J, Hilgarth RS, Kundu K, Murthy N, Kusters D, Reutelingsperger C, Perretti M, Parkos CA, Neish AS and Nusrat A. Annexin A1, formyl peptide receptor, and NOX1 orchestrate epithelial repair. J Clin Invest 2013; 123: 443-454.
[12] Lubrano V and Balzan S. Roles of LOX-1 in microvascular dysfunction. Microvasc Res 2016; 105: 132-140.
[13] Yang H and Li H. CD36 identified by weighted gene co-expression network analysis as a hub candidate gene in lupus nephritis. PeerJ 2019; 7: e7722.
[14] Qiu L and Liu X. Identification of key genes involved in myocardial infarction. Eur J Med Res 2019; 24: 22.
[15] Ritchie ME, Phipson B, Wu D, Hu Y, Law CW, Shi W and Smyth GK. Limma powers differential expression analyses for RNA-sequencing and microarray studies. Nucleic Acids Res 2015; 43: e47.
[16] Botía JA, Vandrovcova J, Forabosco P, Guelfi S, D'Sa K; United Kingdom Brain Expression Consortium, Hardy J, Lewis CM, Ryten M and Weale ME. An additional k-means clustering step improves the biological features of WGCNA gene co-expression networks. BMC Syst Biol 2017; 11: 47.
[17] Vilne B, Skogsberg J, Foroughi Asl H, Talukdar HA, Kessler T, Björkegren JLM and Schunkert H. Network analysis reveals a causal role of mitochondrial gene activity in atherosclerotic lesion formation. Atherosclerosis 2017; 267: 39-48.
[18] Wu YE, Pan L, Zuo Y, Li X and Hong W. Detecting activated cell populations using single-cell RNA-Seq. Neuron 2017; 96: 313-329, e6.
[19] Jang S, Collin de l'Hortet A and Soto-Gutierrez A. Induced pluripotent stem cell-derived endothelial cells: overview, current advances, applications, and future directions. Am J Pathol 2019; 189: 502-512.
[20] Lee DY and Chiu JJ. Atherosclerosis and flow: roles of epigenetic modulation in vascular endothelium. J Biomed Sci 2019; 26: 56.
[21] Poznyak AV, Grechko AV, Orekhova VA, Khotina V, Ivanova EA and Orekhov AN. NADPH oxidases and their role in atherosclerosis. Biomedicines 2020; 8: 206.
[22] Du Y, Chen K, Liu E, Wang X, Li F, Liu T, Zheng X, Li G and Che J. Gender-specific associations of CD36 polymorphisms with the lipid profile and susceptibility to premature multi-vessel coronary artery heart disease in the Northern Han Chinese. Gene 2020; 753: 144806.
[23] The Gene Ontology Consortium. Expansion of the gene ontology knowledgebase and resources. Nucleic Acids Res 2017; 45: D331-D338.
[24] Kanehisa M, Furumichi M, Tanabe M, Sato Y and Morishima K. KEGG: new perspectives on genomes, pathways, diseases and drugs. Nucleic Acids Res 2017; 45: D353-D361.
[25] Ramakrishnan DP, Hajj-Ali RA, Chen Y and Silverstein RL. Extracellular vesicles activate a CD36-dependent signaling pathway to inhibit microvascular endothelial cell migration and tube formation. Arterioscler Thromb Vasc Biol 2016; 36: 534-544.

[26] Magwenzi S, Woodward C, Wraith KS, Aburima A, Raslan Z, Jones H, McNeil C, Wheatcroft S, Yuldasheva N, Febbriao M, Kearney M and Naseem KM. Oxidized LDL activates blood platelets through CD36/NOX2-mediated inhibition of the cGMP/protein kinase G signaling cascade. Blood 2015; 125: 2693-2703.
[27] Liang C, Wang QS, Yang X, Niu N, Hu QQ, Zhang BL, Wu MM, Yu CJ, Chen X, Song BL, Zhang ZR and Ma HP. Oxidized low-density lipoprotein stimulates epithelial sodium channels in endothelial cells of mouse thoracic aorta. Br J Pharmacol 2018; 175: 1318-1328.
[28] Reshetnikov V, Hahn J, Maueröder C, Czegley C, Munoz LE, Herrmann M, Hoffmann MH and Mokhir A. Chemical tools for targeted amplification of reactive oxygen species in neutrophils. Front Immunol 2018; 9: 1827.
[29] Park L, Zhou J, Zhou P, Pistick R, El Jamal S, Younkin L, Pierce J, Arreguin A, Anrather J, Younkin SG, Carlson GA, McEwen BS and Iadecola C. Innate immunity receptor CD36 promotes cerebral amyloid angiopathy. Proc Natl Acad Sci U S A 2013; 110: 3089-3094.
[30] Tondera C, Laube M and Pietzsch J. Insights into binding of S100 proteins to scavenger receptors: class B scavenger receptor CD36 binds S100A12 with high affinity. Amino Acids 2017; 49: 183-191.
[31] Woo MS, Yang J, Beltran C and Cho S. Cell surface CD36 protein in monocyte/macrophage contributes to phagocytosis during the resolution phase of ischemic stroke in mice. J Biol Chem 2016; 291: 23654-23661.
[32] Qin M, Wang L, Li F, Yang M, Song L, Tian F, Yukht A, Shah PK, Rothenberg ME and Sharifi BG. Oxidized LDL activated eosinophil polarize macrophage phenotype from M2 to M1 through activation of CD36 scavenger receptor. Atherosclerosis 2017; 263: 82-91.
[33] Cisternas P, Taylor X and Lasagna-Reeves CA. The amyloid-tau-neuroinflammation axis in the context of cerebral amyloid angiopathy. Int J Mol Sci 2019; 20: 6319.
[34] Son NH, Basu D, Samovski D, Pietka TA, Peche VS, Willecke F, Fang X, Yu SQ, Scerbo D, Chang HR, Sun F, Bagdasarov S, Drosatos K, Yeh ST, Mullick AE, Shoghi KI, Gumaste N, Kim K, Huggins LA, Lhakhang T, Abumrad NA and Goldberg IJ. Endothelial cell CD36 optimizes tissue fatty acid uptake. J Clin Invest 2018; 128: 4329-4342.
[35] Abumrad NA and Goldberg IJ. CD36 actions in the heart: lipids, calcium, inflammation, repair and more? Biochim Biophys Acta 2016; 1861: 1442-1449.
[36] Herb M, Gluschko A and Schramm M. LC3-associated phagocytosis initiated by integrin ITGAM-ITGB2/Mac-1 enhances immunity to Listeria monocytogenes. Autophagy 2018; 14: 1462-1464.
[37] Mayes MD, Bossini-Castillo L, Gorlova O, Martin JE, Zhou X, Chen WV, Assassi S, Ying J, Tan FK, Arnett FC, Reveille JD, Guerra S, Teruel M, Carmona FD, Gregersen PK, Lee AT, López-Isac E, Ochoa E, Carreira P, Simeón CP, Castellví I, González-Gay MÁ; Spanish Scleroderma Group, Zhernakova A, Padyukov L, Alarcón-Riquelme M, Wijmenga C, Brown M, Beretta L, Riemekasten G, Witte T, Hunzelmann N, Kreuter A, Distler JH, Voskuyl AE, Schuerwegh AJ, Hesselstrand R, Nordin A, Airó P, Lunardi C, Shiels P, van Laar JM, Herrick A, Worthington J, Denton C, Wigley FM, Hummers LK, Varga J, Hinchcliff ME, Baron M, Hudson M, Pope JE, Furst DE, Khanna D, Phillips K, Schiopu E, Segal BM, Molitor JA, Silver RM, Steen VD, Simms RW, Lafyatis RA, Fessler BJ, Frech TM, Alkassab F, Docherty P, Kaminska E, Khalidi N, Jones HN, Markland J, Robinson D, Broen J, Radstake TR, Fonseca C, Koeleman BP and Martin J. Immunochip analysis identifies multiple susceptibility loci for systemic sclerosis. Am J Hum Genet 2014; 94: 47-61.
[38] Roberts AL, Thomas ER, Bhosle S, Game L, Obraztsova O, Aitman TJ, Vyse TJ and Rhodes B. Resequencing the susceptibility gene, ITGAM, identifies two functionally deleterious rare variants in systemic lupus erythematosus cases. Arthritis Res Ther 2014; 16: R114.
[39] Gustin A, Kirchmeyer M, Koncina E, Felten P, Losciuto S, Heurtaux T, Tardivel A, Heuschling P and Dostert C. NLRP3 inflammasome is expressed and functional in mouse brain microglia but not in astrocytes. PLoS One 2015; 10: e0130624.
[40] Cattaneo F, Parisi M and Ammendola R. Distinct signaling cascades elicited by different formyl peptide receptor 2 (FPR2) agonists. Int J Mol Sci 2013; 14: 7193-7230.
[41] Abouelasrar Salama S, De Bondt M, De Buck M, Berghmans N, Proost P, Oliveira VLS, Amaral FA, Gouwy M, Van Damme J and Struyf S. Serum amyloid A1 (SAA1) revisited: restricted leukocyte-activating properties of homogeneous SAA1. Front Immunol 2020; 11: 843.
[42] Chen K, Tang P, Bao Z, He T, Xiang Y, Gong W, Yoshimura T, Le Y, Tessarollo L, Chen X and Wang JM. Deficiency in Fpr2 results in reduced numbers of Lin(-)cKit(+)Sca1(+) myeloid progenitor cells. J Biol Chem 2018; 293: 13452-13463.
[43] Petri MH, Laguna-Fernández A, Gonzalez-Diez M, Paulsson-Berne G, Hansson GK and Bäck M. The role of the FPR2/ALX receptor in atherosclerosis development and plaque stability. Cardiovasc Res 2015; 105: 65-74.